

Review

Building towards Supercapacitors with Safer Electrolytes and Carbon Electrodes from Natural Resources

Mohammad Said El Halimi ^{1,2}, Alberto Zanelli ³ , Francesca Soavi ^{1,3,4}  and Tarik Chafik ^{1,*} 

¹ Laboratory of Electrochemistry of Materials for Energetics, Department of Chemistry “Giacomo Ciamician”, Alma Mater Studiorum Università di Bologna, 40126 Bologna, Italy; mohammad.elhalimi@gmail.com (M.S.E.H.); francesca.soavi@unibo.it (F.S.)

² Laboratory of Chemical Engineering and Resources Valorisation, Faculty of Sciences and Techniques of Tangier, Abdelmalek Essaadi University, Tangier 90000, Morocco

³ Institute for Organic Synthesis and Photoreactivity (ISOF), National Research Council (CNR), 40129 Bologna, Italy; alberto.zanelli@isof.cnr.it

⁴ ENERCube—Research Center on Energy, Environment, Sea (CIRI-FRAME), Alma Mater Studiorum Università di Bologna, 48122 Ravenna, Italy

* Correspondence: tchafik@uae.ac.ma

Abstract: The growing interest in energy storage devices, both batteries and capacitors, could lead to the improvement of electrochemical properties such as extended charge/discharge cycles, high specific capacitance, and power density. Furthermore, the use of easily available raw materials for the production of carbon electrodes has attracted interest due to the criticality of the resources related to the current technologies of high-performance capacitors. The present article reviews carbon-based materials for supercapacitors derived from affordable coal deposits or crop waste with appropriate characteristics in terms of specific surface area, electrical conductivity, and charge/discharge stability. In addition, the substitution of organic liquids electrolytes with less dangerous solutions, such as aqueous electrolytes containing high concentrations of salt, is a valuable strategy for the design of green devices that is discussed in this review. Finally, the present article reviews the electrochemical performance of supercapacitors based on carbon electrodes obtained from various natural resources and their compatibility with safer and cheaper electrolytes.

Keywords: energy storage; supercapacitors; natural resources; biomass; coal; carbon-based electrodes; aqueous electrolytes



Citation: El Halimi, M.S.; Zanelli, A.; Soavi, F.; Chafik, T. Building towards Supercapacitors with Safer Electrolytes and Carbon Electrodes from Natural Resources. *World* **2023**, *4*, 431–449. <https://doi.org/10.3390/world4030027>

Academic Editor: Mohammad Aslam Khan Khalil

Received: 20 May 2023

Revised: 3 July 2023

Accepted: 12 July 2023

Published: 14 July 2023



Copyright: © 2023 by the authors. Licensee MDPI, Basel, Switzerland. This article is an open access article distributed under the terms and conditions of the Creative Commons Attribution (CC BY) license (<https://creativecommons.org/licenses/by/4.0/>).

1. Introduction

Currently, more than 70% of the world’s primary energy demand is dominated by fossil fuels. This scenario is expected to change in the near future with the increasing deployment of renewable energy sources as an urgent response to climate change [1]. The alternative energy sources produce energy from sun and wind that typically are not constant [2]. To ensure the reliability and consistency of renewable energy source output, energy storage devices (ESDs) are required as buffers for the intermittent sources. Furthermore, the use of ESDs could power off-grid energy in remote locations [3–5]. Hence, ESDs with high energy and power densities will be crucial in the future to ensure the integration of renewable energy sources into existing power systems and boost the potential for applications related to electric mobility.

ESDs based on batteries and electrochemical supercapacitors (SCs) are in rapid development [6–11]. Lithium-ion batteries have not yet been widely used as an efficient storage technology and still need to overcome some disadvantages, mainly those associated with safety, cost, and metal availability [8,12–15]. SCs have attracted attention in recent years mostly because of their high power density and long life cycle. Notably, these characteristics of SCs allow them to provide interesting hybrid solutions for the automotive sector, where

they are coupled with batteries. Figure 1 shows a Ragone plot with power and energy densities for different electrochemical ESDs and fuel cells for the sake of comparison.

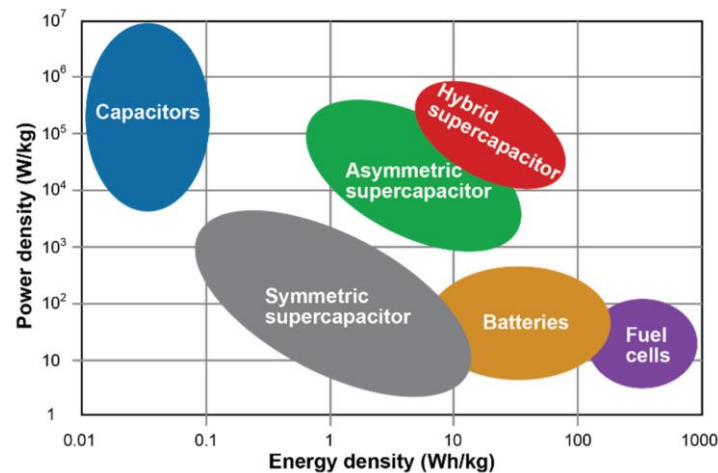


Figure 1. Ragone plot of different ECDs. “Adapted from [16], Copyright (2000), with permission from Elsevier”.

In general, in an electrochemical ESD, the energy storage processes occur at the electrodes either by Faradic or non-Faradic modes. The Faradic processes are controlled by the kinetics and activation energies of the electrode reactions as well as by the mass transport of reagents/products, which limit device power density. In addition, the electrode materials may undergo transformations during cycling, like the modification of the chemical composition or structure. Furthermore, the electrochemical reactions involved may have a columbic efficiency lower than 100%. For these reasons, despite the high charge storage capacity, Faradic electrodes can show reduced lifetimes compared to those involving non-Faradic processes. The latter occur through the electrostatic storage of charges at the electrode surfaces. This phenomenon drives energy storage in electrochemical capacitors. It is a rapid surface phenomenon that is completely reversible and does not yield to any chemical or structural changes in the electrodes. The fast kinetics and high reversibility of the electrostatic process enable high SC power density and a theoretically unlimited lifetime.

2. Supercapacitors (SCs)

SCs, also known as “ultracapacitors”, are used in applications requiring rapid energy storage or high-power delivery [17]. In 1987, they were introduced to the market as small-sized devices for computers [18]. SCs are categorized into the three classes summarized in Figure 2 depending on their mechanism of charge storage [19,20]: electrostatic double-layer capacitors (EDLCs), pseudocapacitors (PC), and hybrid supercapacitors (HSC).

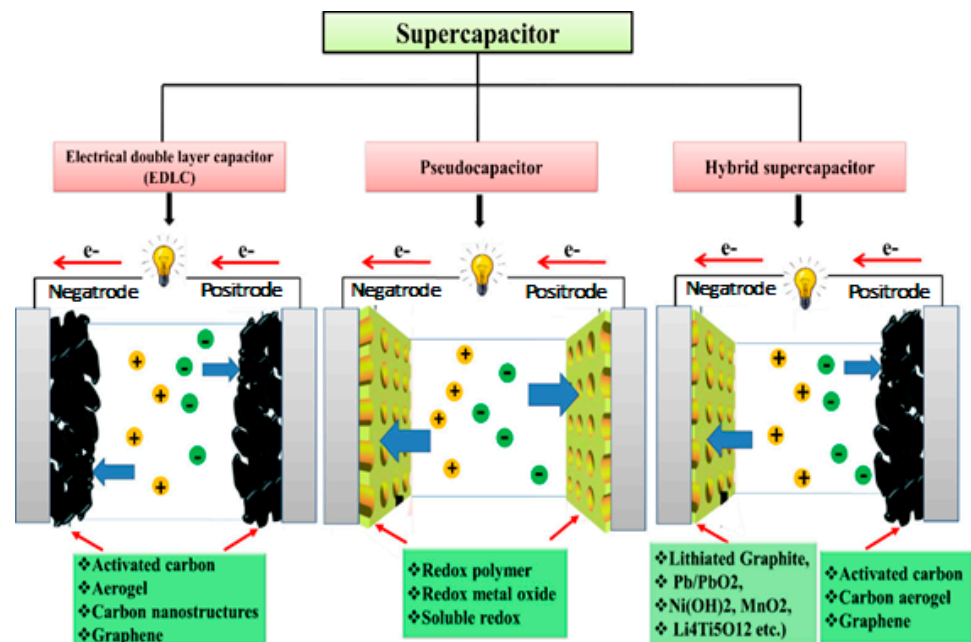


Figure 2. Classification of SCs displaying the used electrode materials and charge storage mechanism. Adapted with permission from [21]. Copyright (2021) American Chemical Society.

2.1. Electrostatic Double-Layer Capacitor (EDLC)

EDLCs are symmetrical SCs featuring two electrodes based on non-electroactive materials. The storage mechanism consists of the accumulation of ions at the electrode/electrolyte interface (capacitive processes) through the creation of an electrochemical double layer (EDL) [22,23]. The EDL has been described by different models, including that of Helmholtz (second half of the 19th century), which simply considers the formation of a layer of ions at the electrode/electrolyte interface, e.g., the formation of anions if the electrode is positively charged (Figure 3a) [24,25]. Guy and Chapman's model (early 20th century) considers the formation of a diffuse layer due to the thermal agitation where the potential decreases exponentially (Figure 3b) [26,27]. Finally, Stern's model (1924) combines these two approaches by forming a compact layer close to the electrode and a diffuse one that extends to the bulk of the solution and is in the order of the nanometers (Figure 3c) [28].

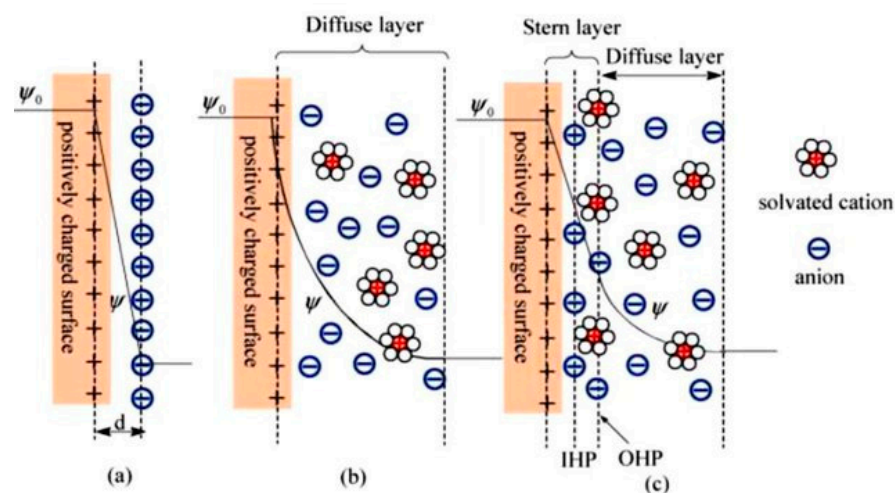


Figure 3. EDL models: (a) Helmholtz [24], (b) Guy–Chapman [27], and (c) Stern [28]. “d” is the EDL distance in Helmholtz model. Ψ_0 and Ψ are the potentials at the electrode surface and electrode/electrolyte interface, respectively [29].

The capacitance (double-layer capacity) depends on the number of ions adsorbed on the electrode and the specific area of the electrode materials for a given potential excursion. One of the most popular materials for EDLCs is carbon due to its good electric conductivity and stability. Furthermore, the material texture of carbon, i.e., its specific surface area (SSA) and pore size distribution, together with the appropriate choice of the electrolyte, greatly affects the SCs electrochemical performance in terms of capacitance and energy density [20]. A number of EDLCs have shown excellent power densities and good cyclic stability, which are associated with fast-charge diffusion in the electrolyte, the negligible side reactions of the different materials, and efficient ion adsorption on the electrode surfaces [22,30].

2.2. Pseudocapacitors (PCs)

PCs electrodes are based mainly on electro-active materials such as metal oxides (e.g., MnO_2 , RuO_2) [31–33] and conjugated polymers (e.g., polypyrroles, polyanilines, and polythiophenes) [34–36]. In these systems, the energy storage mechanism is far more complicated than that of an EDLC, and the charge storage occurs through Faradic charge transfer processes, which are fast and reversible [37]. Regarding inorganic electrode materials, varying the oxidation state of the metal atoms coupled with the insertion/de-insertion of ions in the crystal lattice is the main process. In a recent paper [38], surface-amorphized Co_3S_4 with a capacity higher than 1000 F g^{-1} at 0.5 A g^{-1} in an asymmetric capacitor with carbon-negative electrodes showed a retention rate about 90% after 10,000 cycles.

In the conjugated polymers, the reversible oxidation and reduction in the π - π^* orbitals, coupled with the so-called “doping/de-doping” of the materials by the ions coming from the electrode/electrolyte interface, takes place [39]. Even if the charge/discharge process is not electrostatic like in EDLCs, the electrochemical response under a galvanostatic or voltametric test is similar to that of EDLCs, and for this reason, they are considered PCs [40]. A charge storage comparison between an EDLC and a PC is depicted in Figure 4.

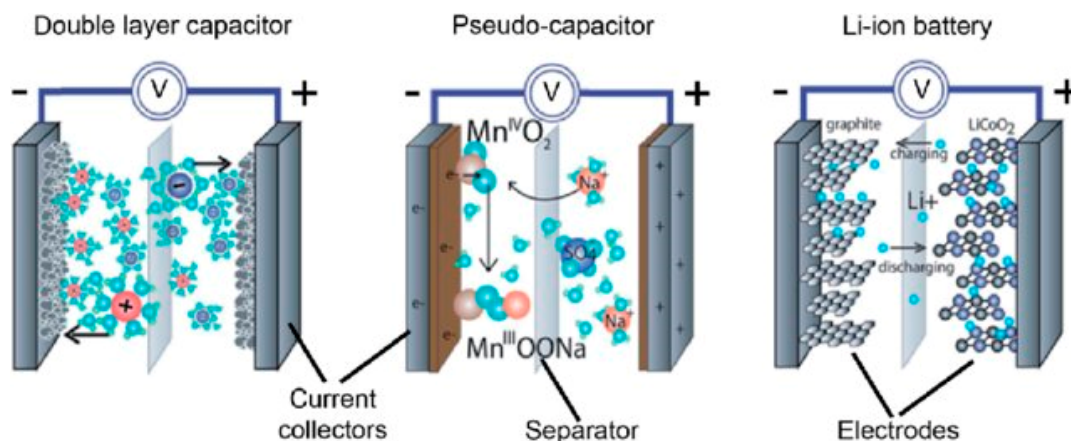


Figure 4. Comparison between ECDLs, PCs, and Li-ion batteries. Adapted from Ref. [41].

Although the capacitance and energy density values that can be increased significantly by utilizing Faradic processes, PCs deliver lower power densities than EDCLs due to the fact that Faradic processes are often slower than non-Faradic ones [42]. Furthermore, the charge storage mechanism, i.e., redox reactions, affects the cycle of PCs because of possible lattice stress phenomena in the transition metal oxides and overoxidation or depolymerization in the conjugated polymers [43,44].

2.3. Hybrid Supercapacitors (HSCs)

HSCs, which are a hybrid of EDLCs and PCs electrodes [45,46], have been designed to obtain SCs with synergistic properties, where the pseudocapacitive electrode makes it possible to obtain a high energy density, and the capacitive electrode enables high power densities. Although PCs and HSCs deliver superior specific capacitance than that of

EDLCs, their potential applications are limited by their lower cycle performance and higher cost [32].

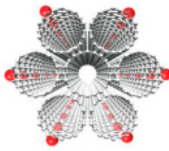
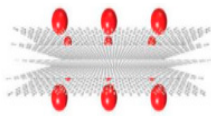
However, researchers are diligently striving towards developing high-specific-capacitance and low-cost EDLCs, which involves advanced active materials for electrodes based on carbon with different structural forms [47]. Also, nanofabrication and coupling with conjugated polymers are widening perspectives in the field, which may lead to improvements in HSC performance [48]. A recent example of an asymmetric HSC was built with a positive electrode of C-coated NiCo_2O_4 on a cactus plant-like three-dimensional Ni structure and a negative electrode based on Fe_3S_4 grown via chemical vapor deposition (CVD) in dendrite-like structures that produce a network on the highly porous Ni-Co alloy obtained via H_2 bubble-assisted electrodeposition on stainless steel. The assembled devices delivered a specific capacitance of 150 F g^{-1} at 1 A g^{-1} and showed 70% of the initial capacitance after 10,000 charge/discharge cycles Swain, et al. [49].

Other metal sulfides coupled with a carbonaceous electrode have been used for asymmetric HSCs with aqueous electrolytes, showing a variety of performances: defect-rich Ni_3S_4-x delivered about 1400 F g^{-1} at 0.1 A g^{-1} without significant capacitance loss after 15,000 cycles [50], whereas Ni-doped SnS_2 on carbon cloth delivered 66 F g^{-1} at 2 A g^{-1} with a capacity retention of 80% [51].

3. Carbon Materials for Supercapacitors

A variety of carbon materials with different morphologies and structures have been used as EDLC electrodes, including activated carbon (AC) obtained from mineral resources or biomasses, carbon nanotubes (CNTs), and graphene, thanks to their large SSA, high porosity, good electronic conductivity, and chemical stability, as well as their wide range of operating temperatures [52]. A comparison of carbon materials for EDLCs is shown in Table 1.

Table 1. Characteristics of carbon materials used as EDLC electrodes. Adapted from Ref. [53].

Material	Carbon Nanotubes	Graphene	Activated Carbon
			
Conductivity	High	High	Structure dependent
Volumetric capacitance	Low	Moderate	High
Cost	High	Moderate	Low

Other synthetic strategies involve the emulsion-assisted production of polymer nanoparticles that, after calcination under N_2 atmosphere, release carbon spheres 200–300 nm in diameter with a single cavity inside and a SSA of about $300 \text{ m}^2 \text{ g}^{-1}$ [54].

The large SSA of carbon is generally responsible for the high specific capacity of the electrode. Large SSAs can reach $2500 \text{ m}^2 \text{ g}^{-1}$ and deliver specific capacitance from 100 to 250 F g^{-1} depending on the electrolyte [55], and, in turn, the pore size distribution significantly affects the EDLC charge/discharge rate. According to the International Union of Pure and Applied Chemistry (IUPAC), the porosity classifications for macropores, mesopores, and micropores are as follows [56]:

- Macropores with a diameter greater than 50 nm;
- Mesopores with a diameter between 2 and 50 nm;
- Micropores with a diameter of less than 2 nm.

It is worth noting that the IUPAC outlines two subcategories of micropores: supermicropores, with diameters between 0.7 nm and 2 nm, and ultramicropores, with diameter less than 0.7 nm [56].

3.1. Activated Carbon (AC)

AC is a promising material for SC electrodes because of its relatively low cost, high conductivity, good thermal stability, and corrosion resistance. Several synthesis routes are for the preparation of activated carbons with high a SSA and a porosity that is suitable for EDLC electrodes have been reported in the literature [57]. It should be emphasized that these characteristics are influenced by the precursor used and the synthesis and activation process [58,59]. Furthermore, activated carbon production processes (carbonization and activation) are generally simple and involve cheap and abundant precursors [60]. The activation process consists of oxidation via physical or chemical processes that allow for the creation of a random network of pores (macropores, mesopores, or micropores). Usually, physical activation is carried out through the carbonization of materials (for biomass or hard coal see below) at temperatures ranging from 900 °C to 1100 °C under oxidizing conditions. Such a temperature range induces the sublimation of the lower molecular weight fraction and structural rearrangement, whereas the oxidation of carbon results in the creation and/or enlargement of the pores.

Chemical activation proceeds in the presence of chemical agents (e.g., H_3PO_4 , ZnCl_2 , KOH , etc.) through the dehydration, carbonization, and structural reorganization of the precursor, inducing the development of micropores and mesopores and the functionalization of their surfaces [61]. By carefully controlling the activation parameters, it is possible to reach a specific surface area of $3000 \text{ m}^2 \cdot \text{g}^{-1}$ [52]. A schematic showing the development of the porosity network can be seen in Figure 5.

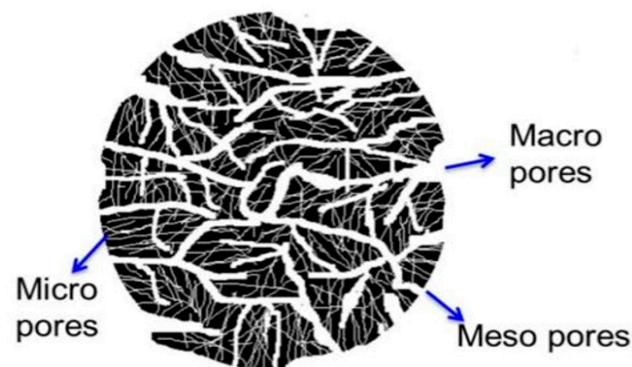


Figure 5. Scheme illustrating the porosity developed in a grain of AC [62].

ACs can be easily produced and, consequently, have been commercially available for a long time for many others applications, including air purification, water treatment, energy storage, etc. Indeed, the global market for AC is growing, and it is expected to be worth up to USD 7 billion by 2028 [63]. From a business point of view, the use of AC is of interest because related low-cost and abundant precursors such as biomass are considered renewable resources; thus, in terms of sustainability, AC production is of great importance.

3.2. Carbon Nanotubes (CNTs)

CNTs have been reported to have special features of interest for EDLC electrodes. The development of high-power SCs has been driven by their high electrical conductivity and accessible pore network, along with their good thermal and mechanical stability [52]. CNTs are classified as single-walled nanotubes (SWCNTs) and multiwalled nanotubes (MWCNTs) based on the number of graphite-like layers rolled into the cylinder, which, in turn, affects the electrical and mechanical characteristics of the resulting materials [52,64]. The main methods for CNTs synthesis are laser ablation, arc-discharge, and CVD, all of which are experimentally complex and require expensive equipment. In addition, it seems difficult to achieve high purity and good bulky yields [57].

3.3. Graphene

Graphene consists of a two-dimensional single-layer of hexagonal rings of sp^2 carbon atoms. This carbon arrangement potentially provides an accessible surface area that is much wider than that of any other carbon material used in EDLCs [52,65]. Graphene can be produced via CVD; chemical [66], electrochemical [67], or plasma exfoliation from natural graphite; and mechanical cleavage from natural graphite [68]. In one study, a graphene ribbon aerogel monolith with high mass loading (11 g cm^{-2}) exhibited a capacitance density of about 150 F g^{-1} at 1 A g^{-1} and about 100% capacitance retention after 10,000 cycles [69].

However, despite their great potential, carbon materials based on graphene or CNTs are still far from being commonly used in industrial sectors, mainly because of their high production costs.

3.4. Activated Biochar-Based SCs

This section of the present article focuses on the use of biomass as a sustainable and renewable precursor for the production of ACs. The fabrication process of biomass-derived AC has been demonstrated by the carbonization and activation of a huge variety of raw materials [70]. During carbonization, biochar is produced as a result of the precursor being subjected to heat treatment in the absence of oxygen. The development of AC surface area and porosity is achieved through physical or chemical activation using oxidizing gases (e.g., O_2 , steam, etc.) or other oxidizing agents (e.g., KOH, NaOH, ZnCl_2 , H_3PO_4), respectively [71–73]. In contrast to physical activation, which partially gasifies the char to CO_2 in order to enhance the pores, chemical activation involves dehydrating chemicals to prevent the development of tar and boost the carbon yield [74]. Chemical activation is sometimes carried out in one step after pyrolysis and sometimes produces AC with a higher carbon yield, larger SSA, and more developed microporosity than physical activation [75].

Using low-cost biomass such as biowaste (e.g., agriculture by-products or food industry waste) to derive ACs for SC electrodes could not only pave the way to solve waste management problems [76,77] but also generate revenue for farmers in the context of circular economy because it changes a waste product in a secondary raw material into a high-value product that could be used to produce SCs [78].

In recent years, interest in producing activated carbon from biomass has steadily grown [78–83]. Various sources of biowaste, including waste from plants, animals, and vegetables, have been listed in the literature as raw materials that could be used to produce ACs for use as electrode materials in SCs [78,84–89]. Figure 6 shows some of those biowaste products, specifically the following: olive seeds, lotus calyx, rice husk, mangosteen peel, chrysopogon zizanioides, lemon peel, eggs shells, and idesia polycarpa fruit oil residue.

For instance, Yang et al. developed a porous carbon with a SSA of $1471.4 \text{ m}^2 \text{ g}^{-1}$ from corncob that provided an EDLC that could deliver an energy density of 20.15 Wh kg^{-1} in 6 M KOH electrolyte [90]. By following the same procedure, Mitravinda et al. investigated EDLCs based on corn silk-derived AC; the EDLCs showed a promising energy density of $\sim 32.28 \text{ Wh kg}^{-1}$ and a power density of 870.68 W kg^{-1} [91]. This was made possible by the AC's mesoporous fiber-like morphology and texture, which helped to diffuse electrolytes into and out of the pores during the charge/discharge processes. In another study, Yin et al. used coconut fibers to develop three-dimensional hierarchical porous carbon [92] with a high SSA of $2898 \text{ m}^2 \text{ g}^{-1}$ and pore volume of $1.59 \text{ cm}^3 \text{ g}^{-1}$ to allow for an EDLC with 6 M KOH to reach an energy density of 53 Wh kg^{-1} and an impressive power density of 8200 W kg^{-1} . Moreover, Qin et al. synthesized pine nutshell-derived AC using physical activation [92], obtaining an interconnected porous structure with different pore size distributions (micro-, meso-, and macropores). This material was used as an electrode in an EDLC with 6 M KOH electrolyte, releasing 98% of the initial capacity after 10,000 cycles [92]. Bridget et al. reported the use of lignin residue from biodigestion plants as a precursor for preparing AC [93]. The lignin-derived carbon contained mesopores and micropores showing a high SSA of $1879 \text{ m}^2 \text{ g}^{-1}$. A SC with this lignin-derived carbon electrode exhibited a specific energy and specific power density of up to 10 Wh kg^{-1} and

6.9 kW kg⁻¹, respectively. Durability tests revealed that the device could maintain 84.5% of its capacitance after 15,000 charge/discharge cycles [93]. Table 2 shows the electrochemical performance of some investigated biowaste-derived carbon electrodes and SCs using aqueous electrolytes.

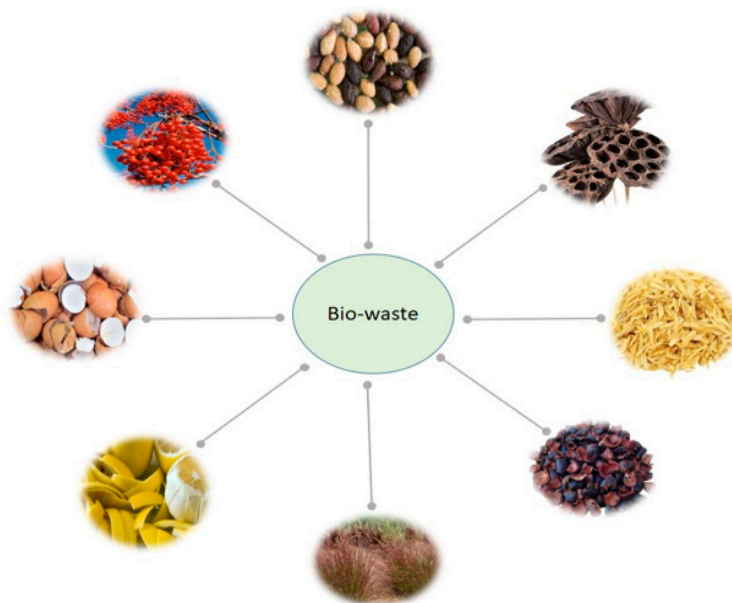


Figure 6. Some biowaste products that could be used as precursors for carbon materials to generate electrodes for SCs.

Table 2. Characteristics of biowaste-derived carbon-based electrodes and the related EDLCs with aqueous electrolytes.

Biowaste	SSA (m ² g ⁻¹)	Specific Capacitance (F/g)	Electrolyte for the Assembled Device	Energy Density (Wh kg ⁻¹)	Power Density (kW kg ⁻¹)	Cyclic Stability (%)	Ref.
Lotus calyx	798	223 (1 A/g)	1 M Na ₂ SO ₄	17.5	0.8	95.5 (10,000)	[94]
Stem pith of helianthus annuus	1900.2	403.6 (0.5 A/g)	6 M KOH	5.8	17.3	94.5 (10,000)	[95]
Mangosteen peel	2623	357 (1 A/g)	1 M Li ₂ SO ₄	17.28	0.401	80 (10,000)	[96]
Lemon peel	744.78	152.14 (1 mV/s)	0.5 M H ₂ SO ₄	4.67	8.113	95.5 (10,000)	[97]
<i>Idesia polycarpa</i> fruit oil residue	1537.1	350.4 (1 A/g)	6 M KOH	6.4	0.1	95.4 (10,000)	[98]
<i>Camellia oleifera</i> shell	1750	259 (1 A/g)	1 M H ₂ SO ₄	8.61	0.477	94 (20,000)	[99]
<i>Syzygium cumini</i>	-	253 (0.5 A/g)	6 M KOH	27.22	0.2	96.5 (5000)	[100]
<i>Chrysopogon zizanioides</i>	-	294 (0.5 A/g)	6 M KOH	16.72	0.2	91.8 (5000)	[100]
Baobab fruit shells	2700.65	332 (1 A/g)	6 M KOH	17.7	166.4	93 (10,000)	[101]

Table 2. Cont.

Biowaste	SSA ($\text{m}^2 \text{g}^{-1}$)	Specific Capacitance (F/g)	Electrolyte for the Assembled Device	Energy Density (Wh kg^{-1})	Power Density (kW kg^{-1})	Cyclic Stability (%)	Ref.
Waste wolfberry fruits	1423	365 (0.2 A/g)	1 M Li_2SO_4	23.2	0.225	96.4 (10,000)	[102]
Camellia pollen	810	300 (1 A/g)	6 M KOH	14.3	-	84.5 (20,000)	[103]
Rice husk	1183	163.1 (0.2 A/g)	6 M KOH	5.1	0.049	85 (6000)	[104]
Corn Husk	1370	127 (1 A/g)	6 M KOH	4.4	0.248	90 (5000)	[105]
Olive Seed	1700	224 (0.25 A/g)	1 M H_2SO_4 / 1 M Na_2SO_4	3–5	20–30	91 (12,500)	[106]
Lignin residue of biodigester	1879	114 (0.5 A/g)	2.5 M KNO_3	10	6.9	84.5 (15,000)	[93]

3.5. Coal-Derived AC-Based SCs

Coal is a low-cost carbon-rich material that exists in large natural reserves. In 2020, global coal reserves were estimated to be 1074 billion tons [107]. Restrictions regarding CO_2 emissions should reduce the use of coal as a fuel and encourage the adoption of other, renewable energy sources with added value due to their applicability to fast-developing zero-emission vehicles [108]. There are five different varieties of coal: peat, lignite, subbituminous, bituminous, and anthracite, all of which are classified according to their carbon content. Peat is a soft, crumbly, dark brown substance formed by the decomposition of dead and partially decaying organic matter on the ground in oxygen-poor conditions. Peat contains the least amount of carbon (less than 60%). Lignite, also known as brown coal, has a brown color and preserves the fibrous aspect of the original wood. Its carbon content varies between 65 and 70%. Subbituminous coal, also known as black lignite, is a dark brown or gray-black coal; its carbon content ranges between 70 and 76%. Anthracite is the most high-quality coal because it contains nearly 95% carbon and has a low moisture content [109]. Figure 7 depicts the typical structures of different coal classes and their degree of coalification.

Similar to biomass-derived AC production, coal derivatives with a large SSA can be obtained by physical activation in the presence of air, O_2 , steam, CO_2 , etc., or by chemical activation using KOH, ZnCl_2 , NaOH, H_3PO_4 , etc. In recent years, many researchers have investigated different coal-based ACs and their performance as SC electrode materials. Zhao et al. [110] used chemical activation by KOH to prepare AC from “hypercoal” with a high surface area of $2540 \text{ m}^2 \text{g}^{-1}$; Zhao et al. reported a capacitance of 46.0 F g^{-1} . Shi et al. [111] assembled a high-performance SC with a specific electrode capacitance of 280 F g^{-1} and energy density of 38.9 Wh kg^{-1} at 0.5 A g^{-1} using an AC produced from anthracite. Zhu et al. [112] prepared high-performance coal derivatives via KOH activation, and the optimized sample had a surface area of $2457 \text{ m}^2 \text{g}^{-1}$ and total pore volume of $1.448 \text{ cm}^3 \text{g}^{-1}$, which allowed the material to exhibit a specific capacitance of 384 F g^{-1} in 6 M KOH.

Table 3 summarizes the electrochemical performance of coal-derived AC electrodes, including specific capacitance and power density values, and EDLCs assembled using aqueous electrolytes. Overall, the use of carbon derived from natural resources presents a propitious opportunity to design affordable, cheap, and environmentally friendly SCs.

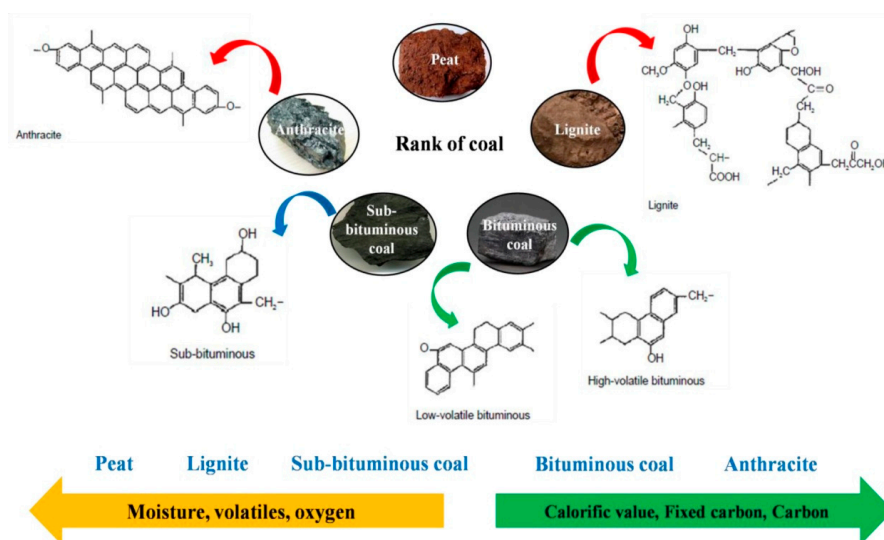


Figure 7. Schematic illustration of different coal classes and their related structural moieties. Reprinted with permission from [21]. Copyright (2021) American Chemical Society.

Table 3. Electrochemical performance of coal-derived carbon-based electrodes (including specific surface area and specific capacitance) and EDLCs (including energy density, power density, and cycling stability) assembled using aqueous electrolytes.

Materials	SSA ($\text{m}^2 \text{g}^{-1}$)	Specific Capacitance (F g^{-1})	Electrolyte for the Assembled Device	Energy Density (Wh kg^{-1})	Power Density (W kg^{-1})	Cyclic Stability (%)	Ref.
Sub-bituminous coal	1021	227 (0.5 A/g)	6 M KOH	25	12.952	82 (10,000)	[113]
Anthracite	3550.7	433 (0.5 A/g)	6 M KOH	38.9	1000	99 (10,000)	[111]
Coal	2129	323 (0.5 A/g)	6 M KOH	10	250	93.7 (10,000)	[114]
Coal tar pitch	3305	308 (1 A/g)	1 M Na_2SO_4	21.9	461.6	-	[115]
Coal tar pitch	3305	308 (1 A/g)	6 M KOH	8.92	254.9	-	[115]
Coal-based green needle coke	807.69	274.9 (1 A/g)	6 M KOH	20.51	1031.42	98.5 (5000)	[116]
Coal tar pitch	2984	320 (0.1 A/g)	6 M KOH	10.6	50.1	94 (10,000)	[117]
Anthracite	2947	282 (0.5 A/g)	6 M KOH	9.75	124.65	-	[118]
Coal	2168	215 (20 A/g)	6 M KOH	7.64	50	91.9 (5000)	[119]
Bituminous coal	3472.41	487 (1 A/g)	6 M KOH	249.6	10.34	96 (10,000)	[120]

4. Electrolytes

The formulation of electrolytes greatly affects the specific performance, environmental impact, and cost of SCs [121]. Several criteria are crucial to consider when choosing an electrolyte, but the two main criteria are the electrochemical stability window (ESW) and the ionic conductivity.

The operating voltage of a SC essentially depends on the electrolyte ESW [17,122]. The conductivity of the electrolyte largely impacts the equivalent series resistance of the SC [123]. The following relation defines the ionic conductivity:

$$k = F \sum_i z_i C_i \mu_i$$

where:

- k is ionic conductivity (S cm^{-1});
- F is the Faraday constant (C mol^{-1});
- z_i is the charge of the ion;
- C_i is the concentration of the ion i (mol cm^{-3});
- μ_i is the mobility of the ion i ($\text{cm}^2 \cdot \text{V}^{-1} \cdot \text{s}^{-1}$).

The operating temperature range of the electrolyte is also a criterion to be taken into account, depending on the intended application of the SC and the related influence on its performance. Furthermore, cost, safety, and environmental impact should also be taken into consideration when choosing an electrolyte [17].

Electrolytes can be categorized into three groups—organic, ionic liquids, and aqueous—each with their own set of advantages and disadvantages (as indicated in Table 4).

Table 4. Comparison of common electrolytes used in supercapacitors [17,124–126].

Electrolyte	Examples	ESW (V)	k (S cm^{-1});	Other Characteristics
Aqueous	H_2SO_4 , KOH, Na_2SO_4 , NH_4Cl	~1.2	High	Cheap, safe, low environmental impact.
Organic	Organic salts (e.g., Et_4NBF_4) in Acetonitrile, propylene carbonate	~3–3.5	Moderate	Flammable, toxic, require low water content (<5 ppm).
Ionic liquid	Imidazolium, pyrrolidinium salts	~4.5	Low	Low flammability, costly.

4.1. Aqueous Electrolytes

Aqueous electrolytes are used in SCs due to their high conductivity, which, for example, can reach up to 700 mS cm^{-1} . In addition, aqueous electrolytes are cheap and relatively environmentally friendly. Unlike organic electrolytes, they do not present a risk of explosion in the case of overheating, and their operating temperature ranges from several degrees below 0°C to about 80°C depending on the nature and the concentration of salt in the water.

The main disadvantage of aqueous electrolytes is their narrow ESW due to the decomposition of water that occurs at the thermodynamic potentials of 1.23 V vs. NHE (oxygen evolution) and 0 V vs. NHE (hydrogen evolution).

However, even with their small ESW, aqueous electrolytes are more promising for use in SCs, at least in the short-term, because of their lower cost, higher safety, lower environmental impact, and higher ionic conductivity compared to that of the other electrolytes [127].

4.2. Organic Electrolytes

At present, probably the most commonly used organic solvents in SC electrolyte solutions are propylene carbonate and acetonitrile. A common salt is tetraethylammonium tetrafluoroborate (Et_4NBF_4). Organic electrolytes make it possible to increase the voltage of a SC up to 2.7 V due to their large ESW. The ionic conductivity of organic electrolytes is lower than that of aqueous electrolytes. In addition, the radiuses of the solvated ions in organic electrolytes are larger than those in water. These two aspects explain why the capacity obtained in organic electrolytes is lower than that obtained in the aqueous ones [128]. In addition, organic electrolytes are costly; also, in some cases they are toxic and may pose safety risks due to vapor tension and their low flash point and heat of combustion.

Even the assembling and recycling process can pose environmental problems due to the leakage of vapors and liquids.

4.3. Ionic Liquids

Ionic liquids are obtained from salts with a melting point below 100 °C and are generally used as liquid electrolytes at room temperature. Notably, no solvent is added. The ions of the salt provide conduction because they are not stuck in a crystal lattice thanks to the large size and asymmetric structure of both the anions and cations. The first ionic liquid, ethylammonium nitrate (EAN), which has a melting point of 12 °C, was described in 1914 by Walden; however, many consider the research on ionic liquids to have really started in the 1970s [129,130]. Among the most investigated ionic liquids are 1-ethyl-3-methylimidazolium bis-(trifluoromethylsulfonyl)-imide (EMITFSI), N-methyl-N-propylpiperidinium bis(trifluoromethanesulfonyl)imide (PP13TFSI), 1-butyl-1-methylpyrrolidinium bis(trifluoromethanesulfonyl)imide (PYR14TFSI), and others [131,132]. Despite their relatively low ionic conductivity and very high cost, ionic liquids are emerging as SC electrolytes because of their non-flammability and high electrochemical and thermal stability [133].

4.4. Water-in-Salt Electrolytes (WiSE)

A remarkable achievement in the development of electrolytic materials has been recently reported by using high-concentration aqueous solutions, known as Water-in-Salt Electrolytes (WiSE), where the low content of water enhances the ESW [134]. In WiSE, the salt content overcomes the solvent both in mass and volume. Because of their very high salt concentration, WiSEs successfully overcome the water's thermodynamic limitations, exhibiting an ESW (about 3.0 V) much larger than what can be achieved with regular aqueous electrolytes while maintaining their intrinsic advantages, such as safety, low cost, environmental friendliness, and satisfactory ionic conductivity. Furthermore, WiSEs enhance the performances of SCs in terms of energy density because they enable higher cell voltages with respect to conventional aqueous solutions [135] (Figure 8).

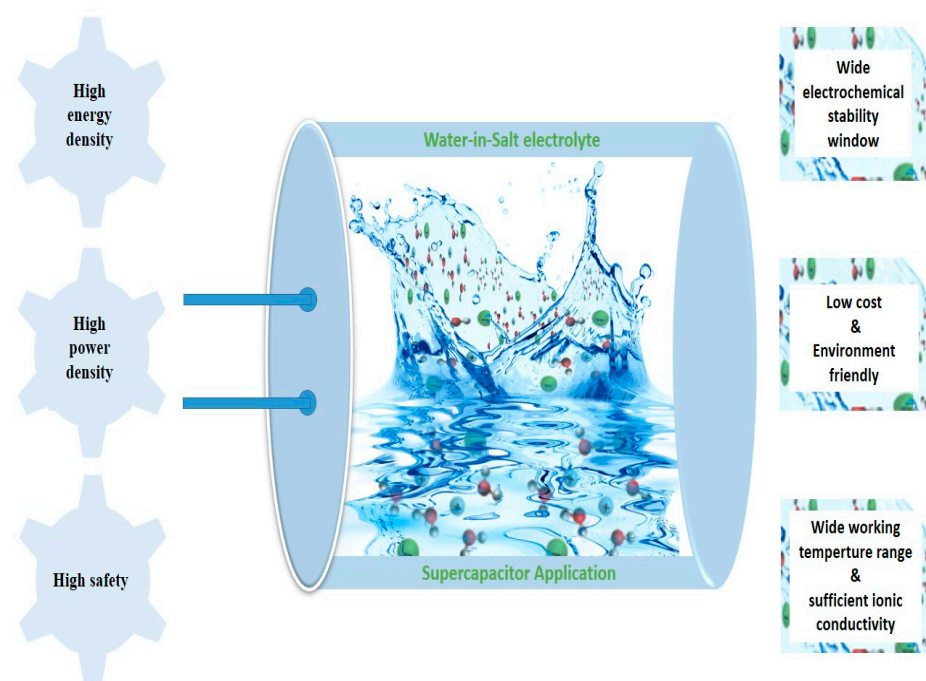


Figure 8. Schematic representation of a WiSE, including its advantages and performance benefits in SC application.

The growing interest in WiSEs for ESDs started in 2015, when, for the first time, Suo et al. revealed a WiSE based on a water and lithium bis(trifluoromethane)-sulfonimide (LiTFSI) with a concentration of 21 mol kg⁻¹, ionic conductivity of 10 mS cm⁻¹, and the capacity to achieve an ESW of 3 V [134]. Until now, fluorinated imide-based salts, notably LiTFSI, are still the most investigated WiSEs for ESDs, including both Li-ion batteries and SCs [136–140]. Despite the tremendous advancements in imide-based WiSE systems, there are some drawbacks related to high costs and negative environmental impacts due to the fluorinated salt, as identified by Lukatskaya et al. for LiTFSI [141]. Moreover, the Li salt quantity required for WiSE has led to concerns associated with Li reserves in the earth's crust, which are less geographically distributed compared with Na and K reserves. However, binary salts, such as eutectic combinations of Li and K acetate, have been proposed as an alternative to reduce the Li content in ESDs. A mixture of 32 mol kg⁻¹ K acetate and 8 mol kg⁻¹ lithium acetate WiSE has been shown to display an ESW of 2.7 V and ionic conductivity 5.3 mS cm⁻¹ [141]. Furthermore, EDLCs enable the use of lithium-free WiSE, and potassium acetate-based WiSEs coupled with AC electrodes have been exploited to produce a SC with a very good cycle life at an operational voltage of 2 V [142].

WiSEs based on percholate salts have also shown excellent properties for EDLCs; however, this type of WiSE could not be regarded as completely green due to the strong oxidizing characteristics of perchlorate anions making it potentially explosive [143].

Unfortunately, superconcentrated acetate solutions are intrinsically alkaline because of acetate anions' hydrolysis reaction, but mild neutral electrolytes based on a low-cost Na perchlorate WiSE can achieve an ionic conductivity of 64.2 mS cm⁻¹ and an ESW of 2.8 V, enabling EDLCs with an operating voltage of 2.3 V [136]. Recently, a study was conducted to investigate a safer and less corrosive circumneutral WiSE prepared from a superconcentrated aqueous solution of ammonium acetate that shows a pH in the range 7–8 and an ionic conductivity that is comparable to or higher than that of typical organic electrolytes [144]. Molecular dynamic simulations gave an atomic-level view of the system; the solution's structural changes at high concentrations, induced by intense interactions with both ions and/or molecules of water accompanying the hydrogen bonding formation, causes an increase in pH and a decrease in ion mobility. Furthermore, molecular dynamic simulation revealed that, moving from conventional solutions to concentrated solutions, the mixture moves from an "ion in water" to an "ionic-liquid-like" behavior [144]. The 26.4 mol kg⁻¹ WiSE of ammonium acetate exhibited an ESW of 2.22 V at Al foil, 2.9 V at glassy carbon, and a remarkable value of 3.4 V at Ti grid. Then, a SC was assembled using this WiSE and AC electrodes prepared from Argan shell. The device showed excellent specific capacitance, low resistance, a cell voltage of 1.2 V, and operative temperatures ranging from -10 °C to +80 °C [144]. The combination of WiSEs and AC electrodes derived from natural resources can pave the way for a new generation of sustainable SCs that are intrinsically safe and have performances comparable to those derived from organic solutions.

5. Summary

The present review discussed novel electrode materials, alternative electrolytes, and the storage mechanisms governing SCs, particularly regarding the use of AC electrodes obtained from widely available and low-cost raw materials. The compatibility of these electrodes with aqueous electrolytes and related advantages have been highlighted in terms of safety and electrochemical performance. The characteristics of AC obtained from abundant natural resources regarding structural and textural properties, interconnected porous structure, and micro- and mesopore size distribution have been discussed with respect to related electrochemical properties. Such characteristics make these materials compatible with aqueous electrolytes with high salt concentrations. These solutions, known as WiSEs, show an ESW up to 3 V, paving the way for the development of aqueous SCs with high cell voltages and high energy densities. Some WiSEs based on low-cost salts such as K acetate, Na perchlorate, and ammonium acetate are comparable to LiTFSI-based

WiSEs. These low-cost WiSE systems show performances that are comparable to or even superior than LiTFSI-based WiSEs, helping to reduce costs, preserve the environment, and, as a result, showing promise for deployment on a commercial level.

Author Contributions: M.S.E.H.: Conceptualization, Writing—original draft. A.Z.: Writing—revising, editing, and reviewing. Funding acquisition, Project administration. F.S.: Conceptualization, Writing original draft, Writing—review and editing, Supervision, Funding acquisition, Project administration. T.C.: Conceptualization, Writing—original draft, Writing—review and editing, Supervision, Funding acquisition, Project administration. All authors have read and agreed to the published version of the manuscript.

Funding: This research was funded by The bilateral project CNR Italy CNRST Morocco “Green Supercapacitors” (SAC.AD002.014, n. 7974, C.U.P. B54I20 0 0 0790 0 05) and the PPR2 16/17 project CNRST Morocco. M.S acknowledges the Italian Ministry of Foreign Affairs and International Cooperation (MAECI) grant program (MAECI-IRE, grant 20/21). F.S acknowledges The European Union’s Horizon 2020 HyFlow Project (agreement No 963550).

Institutional Review Board Statement: Not applicable.

Informed Consent Statement: Not applicable.

Data Availability Statement: No new data were created or analyzed in this study. Data sharing is not applicable to this article.

Conflicts of Interest: The authors declare no conflict of interest.

References

- Dias, R.A.; Mattos, C.R.; Balestieri, J.A. The limits of human development and the use of energy and natural resources. *Energy Policy* **2006**, *34*, 1026–1031. [[CrossRef](#)]
- Sovacool, B.K. The intermittency of wind, solar, and renewable electricity generators: Technical barrier or rhetorical excuse? *Util. Policy* **2009**, *17*, 288–296. [[CrossRef](#)]
- El Shahat, A.; Keyhani, A. Sizing high speed micro generators for smart grid systems. In *Smart Power Grids 2011*; Springer: Berlin/Heidelberg, Germany, 2012; pp. 177–234.
- Ponds, K.T.; Arefi, A.; Sayigh, A.; Ledwich, G. Aggregator of demand response for renewable integration and customer engagement: Strengths, weaknesses, opportunities, and threats. *Energies* **2018**, *11*, 2391. [[CrossRef](#)]
- Cao, W. Biomass-Derived Activated Carbons for Electrical Double Layer Supercapacitors: Performance and Stress Effect. Ph.D. Dissertation, University of Kentucky, Lexington, KY, USA, 2019.
- Afif, A.; Rahman, S.M.; Azad, A.T.; Zaini, J.; Islan, M.A.; Azad, A.K. Advanced materials and technologies for hybrid supercapacitors for energy storage—A review. *J. Energy Storage* **2019**, *25*, 100852. [[CrossRef](#)]
- Luo, B.; Ye, D.; Wang, L. Recent progress on integrated energy conversion and storage systems. *Adv. Sci.* **2017**, *4*, 1700104. [[CrossRef](#)]
- Gallo, A.; Simões-Moreira, J.; Costa, H.; Santos, M.; Dos Santos, E.M. Energy storage in the energy transition context: A technology review. *Renew. Sustain. Energy Rev.* **2016**, *65*, 800–822. [[CrossRef](#)]
- Dhimish, M.; Schofield, N. Single-switch boost-buck DC-DC converter for industrial fuel cell and photovoltaics applications. *Int. J. Hydrogen Energy* **2021**, *47*, 1241–1255. [[CrossRef](#)]
- Kamel, A.A.; Rezk, H.; Abdelkareem, M.A. Enhancing the operation of fuel cell-photovoltaic-battery-supercapacitor renewable system through a hybrid energy management strategy. *Int. J. Hydrogen Energy* **2021**, *46*, 6061–6075. [[CrossRef](#)]
- Thounthong, P.; Chunkag, V.; Sethakul, P.; Sikkabut, S.; Pierfederici, S.; Davat, B. Energy management of fuel cell/solar cell/supercapacitor hybrid power source. *J. Power Source* **2011**, *196*, 313–324. [[CrossRef](#)]
- Choi, J.W.; Aurbach, D. Promise and reality of post-lithium-ion batteries with high energy densities. *Nat. Rev. Mater.* **2016**, *1*, 16013. [[CrossRef](#)]
- Kim, T.; Song, W.; Son, D.-Y.; Ono, L.K.; Qi, Y. Lithium-ion batteries: Outlook on present, future, and hybridized technologies. *J. Mater. Chem. A* **2019**, *7*, 2942–2964. [[CrossRef](#)]
- Chen, T.; Jin, Y.; Lv, H.; Yang, A.; Liu, M.; Chen, B.; Xie, Y.; Chen, Q. Applications of lithium-ion batteries in grid-scale energy storage systems. *Trans. Tianjin Univ.* **2020**, *26*, 208–217. [[CrossRef](#)]
- Nishi, Y. Lithium ion secondary batteries; past 10 years and the future. *J. Power Source* **2001**, *100*, 101–106. [[CrossRef](#)]
- Vandeginste, V. A review of fabrication technologies for carbon electrode-based micro-supercapacitors. *Appl. Sci.* **2022**, *12*, 862. [[CrossRef](#)]
- Smith, B.; Wills, R.; Cruden, A. Aqueous Al-ion cells and supercapacitors—A comparison. *Energy Rep.* **2020**, *6*, 166–173. [[CrossRef](#)]
- Miller, J.R.; Simon, P. Electrochemical capacitors for energy management. *Sci. Mag.* **2008**, *321*, 651–652. [[CrossRef](#)]
- Kötz, R.; Carlen, M. Principles and applications of electrochemical capacitors. *Electrochim. Acta* **2000**, *45*, 2483–2498. [[CrossRef](#)]

20. Conway, B.E. *Electrochemical Supercapacitors: Scientific Fundamentals and Technological Applications*; Springer Science & Business Media: Berlin/Heidelberg, Germany, 2013.
21. Bora, M.; Bhattacharjya, D.; Saikia, B.K. Coal-Derived Activated Carbon for Electrochemical Energy Storage: Status on Supercapacitor, Li-Ion Battery, and Li-S Battery Applications. *Energy Fuels* **2021**, *35*, 18285–18307. [[CrossRef](#)]
22. Simon, P.; Gogotsi, Y. Materials for electrochemical capacitors. In *Nanoscience and Technology: A Collection of Reviews from Nature Journals*; World Scientific: Singapore, 2010; pp. 320–329.
23. Salanne, M.; Rotenberg, B.; Naoi, K.; Kaneko, K.; Taberna, P.-L.; Grey, C.P.; Dunn, B.; Simon, P. Efficient storage mechanisms for building better supercapacitors. *Nat. Energy* **2016**, *1*, 16070. [[CrossRef](#)]
24. Helmholtz, H.V. Ueber einige Gesetze der Vertheilung elektrischer Ströme in körperlichen Leitern, mit Anwendung auf die thierisch-elektrischen Versuche (Schluss.). *Ann. Phys.* **1853**, *165*, 353–377. [[CrossRef](#)]
25. Bockris, J.; Reddy, A.M. *Gamboa-Aldeco in: Modern Electrochemistry Vol. 2A*; Kluwer Academic/Plenum Publishers: New York, NY, USA, 2000.
26. Guoy, G. Constitution of the electric charge at the surface of an electrolyte. *J. Phys.* **1910**, *9*, 457–467.
27. Grahame, D.C. The electrical double layer and the theory of electrocapillarity. *Chem. Rev.* **1947**, *41*, 441–501. [[CrossRef](#)] [[PubMed](#)]
28. Stern, O. The theory of the electrolytic double-layer. *Z. Elektrochem.* **1924**, *30*, 1014–1020.
29. Luo, X.-Y.; Chen, Y.; Mo, Y. A review of charge storage in porous carbon-based supercapacitors. *New Carbon Mater.* **2021**, *36*, 49–68. [[CrossRef](#)]
30. Goel, P.; Sundriyal, S.; Shrivastav, V.; Mishra, S.; Dubal, D.P.; Kim, K.-H.; Deep, A. Perovskite materials as superior and powerful platforms for energy conversion and storage applications. *Nano Energy* **2021**, *80*, 105552. [[CrossRef](#)]
31. Wang, Y.; Guo, J.; Wang, T.; Shao, J.; Wang, D.; Yang, Y.-W. Mesoporous transition metal oxides for supercapacitors. *Nanomaterials* **2015**, *5*, 1667–1689. [[CrossRef](#)]
32. Dubal, D.P.; Gómez-Romero, P.; Korotcenkov, G. *Metal Oxides in Supercapacitors*; Elsevier: Amsterdam, The Netherlands, 2017.
33. Karbak, M.; Boujibar, O.; Lahmar, S.; Ah-Lung, G.; Autret-Lambert, C.; Chafik, T.; Ghamouss, F. Nanometric MnO₂ and MnO₂-Graphene Oxide Materials Enabled by a Solvent-Assisted Synthesis and Their Application in Asymmetric Supercapacitors. *Energy Technol.* **2023**, *11*, 2201243. [[CrossRef](#)]
34. Prasad, K.R.; Munichandraiah, N. Fabrication and evaluation of 450 F electrochemical redox supercapacitors using inexpensive and high-performance, polyaniline coated, stainless-steel electrodes. *J. Power Source* **2002**, *112*, 443–451. [[CrossRef](#)]
35. Clemente, A.; Panero, S.; Spila, E.; Scrosati, B. Solid-state, polymer-based, redox capacitors. *Solid State Ion.* **1996**, *85*, 273–277. [[CrossRef](#)]
36. Mastragostino, M.; Paraventi, R.; Zanelli, A. Supercapacitors based on composite polymer electrodes. *J. Electrochem. Soc.* **2000**, *147*, 3167. [[CrossRef](#)]
37. Augustyn, V.; Simon, P.; Dunn, B. Pseudocapacitive oxide materials for high-rate electrochemical energy storage. *Energy Environ. Sci.* **2014**, *7*, 1597–1614. [[CrossRef](#)]
38. Wang, H.Y.; Liang, M.M.; Ma, H.; Zhang, H.M.; Guo, Z.; Zhao, Y.; Zhao, Y.Z.; RehmanLashari, N.U.; Miao, Z.C. Enhanced cycling performance of surface-amorphized Co₃S₄ as robust cathode for supercapacitors. *J. Energy Storage* **2023**, *58*, 106322. [[CrossRef](#)]
39. Majumdar, D.; Maiyalagan, T.; Jiang, Z. Recent progress in ruthenium oxide-based composites for supercapacitor applications. *ChemElectroChem* **2019**, *6*, 4343–4372. [[CrossRef](#)]
40. Brousse, T.; Bélanger, D.; Long, J.W. To be or not to be pseudocapacitive? *J. Electrochem. Soc.* **2015**, *162*, A5185. [[CrossRef](#)]
41. Jost, K.; Dion, G.; Gogotsi, Y. Textile energy storage in perspective. *J. Mater. Chem. A* **2014**, *2*, 10776–10787. [[CrossRef](#)]
42. Conway, B.E.; Birss, V.; Wojtowicz, J. The role and utilization of pseudocapacitance for energy storage by supercapacitors. *J. Power Source* **1997**, *66*, 1–14. [[CrossRef](#)]
43. Samantara, A.K.; Ratha, S. *Materials Development for Active/Passive Components of a Supercapacitor: Background, Present Status and Future Perspective*; Springer: Berlin/Heidelberg, Germany, 2017.
44. Sundriyal, S.; Kaur, H.; Bhardwaj, S.K.; Mishra, S.; Kim, K.-H.; Deep, A. Metal-organic frameworks and their composites as efficient electrodes for supercapacitor applications. *Coord. Chem. Rev.* **2018**, *369*, 15–38. [[CrossRef](#)]
45. Wang, Y.; Song, Y.; Xia, Y. Electrochemical capacitors: Mechanism, materials, systems, characterization and applications. *Chem. Soc. Rev.* **2016**, *45*, 5925–5950. [[CrossRef](#)]
46. Vangari, M.; Pryor, T.; Jiang, L. Supercapacitors: Review of materials and fabrication methods. *J. Energy Eng.* **2013**, *139*, 72–79. [[CrossRef](#)]
47. Wu, N.; Bai, X.; Pan, D.; Dong, B.; Wei, R.; Naik, N.; Patil, R.R.; Guo, Z. Recent advances of asymmetric supercapacitors. *Adv. Mater. Interfaces* **2021**, *8*, 2001710. [[CrossRef](#)]
48. Peng, H.; Zheng, Y.; Antheaume, C.; Samori, P.; Ciesielski, A. Novel thiophene-based donor–acceptor scaffolds as cathodes for rechargeable aqueous zinc-ion hybrid supercapacitors. *Chem. Commun.* **2022**, *58*, 6689–6692. [[CrossRef](#)] [[PubMed](#)]
49. Swain, N.; Balasubramaniam, S.; Ramadoss, A. High energy density supercapattery empowered by efficient binder-free three-dimensional carbon coated NiCo₂O₄/Ni battery and Fe₃S₄@NiCo pseudocapacitive electrodes. *J. Energy Storage* **2023**, *58*, 106220. [[CrossRef](#)]
50. Wang, H.; Liang, M.; Ma, H.; Zhang, H.; Ma, C.; Duan, W.; Zhao, Y.; Miao, Z. Defect-rich Ni₃S₄–x as a robust electrode material for supercapacitor and aqueous Ni-Zn battery applications. *J. Alloys Compd.* **2023**, *933*, 167733. [[CrossRef](#)]

51. Liang, M.; Li, X.; Kang, Y.; ur RehmanLashari, N.; Zhang, X.; Zhao, Y.; Wang, H.; Miao, Z.; Fu, C. Ni-doped tin disulfide@ Nickel hydroxide as robust cathode toward durable supercapacitor and aqueous Ni-Zn battery. *J. Power Source* **2022**, *535*, 231486. [CrossRef]
52. Kang, J.H. Fabrication and Characterization of Nano Carbon-Based Electrochemical Double-Layer Capacitors. Ph.D. Thesis, University of Waterloo, Waterloo, ON, Canada, 2015.
53. Cheng, Q.; Tang, J.; Ma, J.; Zhang, H.; Shinya, N.; Qin, L.-C. Graphene and carbon nanotube composite electrodes for supercapacitors with ultra-high energy density. *Phys. Chem. Chem. Phys.* **2011**, *13*, 17615–17624. [CrossRef]
54. Liu, Y.; Li, L.; Zhang, L.; Han, G.; Liu, Z.; Huang, J.; Zhang, L.; Luo, J.; Zhu, Z.; Qiao, Z.A. Emulsion-assisted interfacial polymerization strategy: Controllable architectural engineering of anisotropic and isotropic nanoparticles for high-performance supercapacitors. *Battery Energy* **2023**, *2*, 20220058. [CrossRef]
55. Bizuneh, G.G.; Adam, A.M.; Ma, J. Progress on carbon for electrochemical capacitors. *Battery Energy* **2023**, *2*, 20220021. [CrossRef]
56. Rouquerol, J.; Avnir, D.; Fairbridge, C.; Everett, D.; Haynes, J.; Pernicone, N.; Ramsay, J.; Sing, K.; Unger, K. Recommendations for the characterization of porous solids (Technical Report). *Pure Appl. Chem.* **1994**, *66*, 1739–1758. [CrossRef]
57. Wei, L.; Yushin, G. Nanostructured activated carbons from natural precursors for electrical double layer capacitors. *Nano Energy* **2012**, *1*, 552–565. [CrossRef]
58. Boujibar, O.; Ghamouss, F.; Ghosh, A.; Achak, O.; Chafik, T. Activated carbon with exceptionally high surface area and tailored nanoporosity obtained from natural anthracite and its use in supercapacitors. *J. Power Source* **2019**, *436*, 226882. [CrossRef]
59. Boujibar, O.; Ghosh, A.; Achak, O.; Chafik, T.; Ghamouss, F. A high energy storage supercapacitor based on nanoporous activated carbon electrode made from Argan shells with excellent ion transport in aqueous and non-aqueous electrolytes. *J. Energy Storage* **2019**, *26*, 100958. [CrossRef]
60. Chafik, T. Nanoporous Carbonated Materials Prepared from the Shell of the Argan Fruit 1–14. WO2012050411A1, 19 April 2012.
61. Molina-Sabio, M.; Rodriguez-Reinoso, F. Role of chemical activation in the development of carbon porosity. *Colloids Surf. A Physicochem. Eng. Asp.* **2004**, *241*, 15–25. [CrossRef]
62. Strand, G. *Activated Carbon for Purification of Alcohol*; Gert Strand AB: Malmoe, Sweden, 2001.
63. Markets and Markets. Available online: <https://www.researchandmarkets.com/reports/4040498/activated-carbon-market-by-type-powdered> (accessed on 20 May 2023).
64. Moreira, J.V.S.; Corat, E.J.; May, P.W.; Cardoso, L.D.R.; Lelis, P.A.; Zanin, H. Freestanding aligned multi-walled carbon nanotubes for supercapacitor devices. *J. Electron. Mater.* **2016**, *45*, 5781–5788. [CrossRef]
65. Karbak, M.; Boujibar, O.; Lahmar, S.; Autret-Lambert, C.; Chafik, T.; Ghamouss, F. Chemical Production of graphene oxide with high surface energy for supercapacitor applications. *C* **2022**, *8*, 27. [CrossRef]
66. Xia, Z.Y.; Pezzini, S.; Treossi, E.; Giambastiani, G.; Corticelli, F.; Morandi, V.; Zaneli, A.; Bellani, V.; Palermo, V. The Exfoliation of Graphene in Liquids by Electrochemical, Chemical, and Sonication-Assisted Techniques: A Nanoscale Study. *Adv. Funct. Mater.* **2013**, *23*, 4684–4693. [CrossRef]
67. Xia, Z.Y.; Giambastiani, G.; Christodoulou, C.; Nardi, M.V.; Koch, N.; Treossi, E.; Bellani, V.; Pezzini, S.; Corticelli, F.; Morandi, V.; et al. Synergic Exfoliation of Graphene with Organic Molecules and Inorganic Ions for the Electrochemical Production of Flexible Electrodes. *Chempluschem* **2014**, *79*, 439–446. [CrossRef] [PubMed]
68. Cheaptubes. Available online: <https://www.cheaptubes.com/graphene-synthesis-properties-and-applications/> (accessed on 20 May 2023).
69. Wang, D.; Sheng, L.; Jiang, M.; Jin, X.; Lin, X.; Lee, S.Y.; Shi, J.; Chen, W. Density and porosity optimization of graphene monoliths with high mass-loading for high-volumetric-capacitance electrodes. *Battery Energy* **2022**, *1*, 20220017. [CrossRef]
70. Azam, M.A.; Ramli, N.S.N.; Nor, N.A.N.M.; Nawi, T.I.T. Recent advances in biomass-derived carbon, mesoporous materials, and transition metal nitrides as new electrode materials for supercapacitor: A short review. *Int. J. Energy Res.* **2021**, *45*, 8335–8346. [CrossRef]
71. Mestre, A.S.; Carvalho, A.P. Nanoporous carbon synthesis: An old story with exciting new chapters. In *Porosity*; Ghrib, T., Ed.; IntechOpen: London, UK, 2018; pp. 37–68.
72. Idris-Hermann, K.T.; Raoul, T.T.D.; Giscard, D.; Gabche, A.S. Preparation and characterization of activated carbons from bitter kola (*Garcinia kola*) nut shells by chemical activation method using H₃PO₄; KOH and ZnCl₂. *Chem. Sci. Int. J.* **2018**, *23*, 1–15. [CrossRef]
73. Jiang, L.; Sheng, L.; Fan, Z. Biomass-derived carbon materials with structural diversities and their applications in energy storage. *Sci. China Mater.* **2018**, *61*, 133–158. [CrossRef]
74. Williams, P.T.; Reed, A.R. Development of activated carbon pore structure via physical and chemical activation of biomass fibre waste. *Biomass Bioenergy* **2006**, *30*, 144–152. [CrossRef]
75. Şentorun-Shalaby, Ç.D.; Uçak-Astarlıoğlu, M.G.; Artok, L.; Sarıcı, Ç. Preparation and characterization of activated carbons by one-step steam pyrolysis/activation from apricot stones. *Microporous Mesoporous Mater.* **2006**, *88*, 126–134. [CrossRef]
76. Zhang, L.; Liu, Z.; Cui, G.; Chen, L. Biomass-derived materials for electrochemical energy storages. *Prog. Polym. Sci.* **2015**, *43*, 136–164. [CrossRef]
77. Ayinla, R.T.; Dennis, J.; Zaid, H.; Sanusi, Y.; Usman, F.; Adebayo, L. A review of technical advances of recent palm bio-waste conversion to activated carbon for energy storage. *J. Clean. Prod.* **2019**, *229*, 1427–1442. [CrossRef]

78. Sundriyal, S.; Shrivastav, V.; Pham, H.D.; Mishra, S.; Deep, A.; Dubal, D.P. Advances in bio-waste derived activated carbon for supercapacitors: Trends, challenges and prospective. *Resour. Conserv. Recycl.* **2021**, *169*, 105548. [[CrossRef](#)]
79. Guo, Z.; Yan, N.; Lapkin, A.A. Towards circular economy: Integration of bio-waste into chemical supply chain. *Curr. Opin. Chem. Eng.* **2019**, *26*, 148–156. [[CrossRef](#)]
80. Dugmore, T.I.; Clark, J.H.; Bustamante, J.; Houghton, J.A.; Matharu, A.S. Valorisation of biowastes for the production of green materials using chemical methods. In *Chemistry and Chemical Technologies in Waste Valorization*; Springer: Berlin/Heidelberg, Germany, 2017; pp. 73–121.
81. Yahya, M.A.; Al-Qodah, Z.; Ngah, C.Z. Agricultural bio-waste materials as potential sustainable precursors used for activated carbon production: A review. *Renew. Sustain. Energy Rev.* **2015**, *46*, 218–235. [[CrossRef](#)]
82. Liu, S.; Ge, L.; Gao, S.; Zhuang, L.; Zhu, Z.; Wang, H. Activated carbon derived from bio-waste hemp hurd and retted hemp hurd for CO₂ adsorption. *Compos. Commun.* **2017**, *5*, 27–30. [[CrossRef](#)]
83. Manasa, P.; Lei, Z.J.; Ran, F. Biomass waste derived low cost activated carbon from carchorus olitorius (Jute fiber) as sustainable and novel electrode material. *J. Energy Storage* **2020**, *30*, 101494. [[CrossRef](#)]
84. Raj, C.J.; Rajesh, M.; Manikandan, R.; Yu, K.H.; Anusha, J.; Ahn, J.H.; Kim, D.-W.; Park, S.Y.; Kim, B.C. High electrochemical capacitor performance of oxygen and nitrogen enriched activated carbon derived from the pyrolysis and activation of squid gladius chitin. *J. Power Source* **2018**, *386*, 66–76. [[CrossRef](#)]
85. Na, R.; Wang, X.; Lu, N.; Huo, G.; Lin, H.; Wang, G. Novel egg white gel polymer electrolyte and a green solid-state supercapacitor derived from the egg and rice waste. *Electrochim. Acta* **2018**, *274*, 316–325. [[CrossRef](#)]
86. Gong, C.; Wang, X.; Ma, D.; Chen, H.; Zhang, S.; Liao, Z. Microporous carbon from a biological waste-stiff silkworm for capacitive energy storage. *Electrochim. Acta* **2016**, *220*, 331–339. [[CrossRef](#)]
87. Rawal, S.; Joshi, B.; Kumar, Y. Synthesis and characterization of activated carbon from the biomass of *Saccharum bengalense* for electrochemical supercapacitors. *J. Energy Storage* **2018**, *20*, 418–426. [[CrossRef](#)]
88. Su, X.-L.; Li, S.-H.; Jiang, S.; Peng, Z.-K.; Guan, X.-X.; Zheng, X.-C. Superior capacitive behavior of porous activated carbon tubes derived from biomass waste-cotonier strobili fibers. *Adv. Powder Technol.* **2018**, *29*, 2097–2107. [[CrossRef](#)]
89. Song, M.; Zhou, Y.; Ren, X.; Wan, J.; Du, Y.; Wu, G.; Ma, F. Biowaste-based porous carbon for supercapacitor: The influence of preparation processes on structure and performance. *J. Colloid Interface Sci.* **2019**, *535*, 276–286. [[CrossRef](#)]
90. Yang, S.; Zhang, K. Converting corncob to activated porous carbon for supercapacitor application. *Nanomaterials* **2018**, *8*, 181. [[CrossRef](#)] [[PubMed](#)]
91. Mitravinda, T.; Nanaji, K.; Anandan, S.; Jyothirmayi, A.; Chakravadhanula, V.S.K.; Sharma, C.S.; Rao, T.N. Facile synthesis of corn silk derived nanoporous carbon for an improved supercapacitor performance. *J. Electrochem. Soc.* **2018**, *165*, A3369. [[CrossRef](#)]
92. Yin, L.; Chen, Y.; Zhao, X.; Hou, B.; Cao, B. 3-Dimensional hierarchical porous activated carbon derived from coconut fibers with high-rate performance for symmetric supercapacitors. *Mater. Des.* **2016**, *111*, 44–50. [[CrossRef](#)]
93. Mutuma, B.K.; Sylla, N.F.; Bubu, A.; Ndiaye, N.M.; Santoro, C.; Brilloni, A.; Poli, F.; Manyala, N.; Soavi, F. Valorization of biodigester plant waste in electrodes for supercapacitors and microbial fuel cells. *Electrochim. Acta* **2021**, *391*, 138960. [[CrossRef](#)]
94. Dhakal, G.; Mohapatra, D.; Kim, Y.-I.; Lee, J.; Kim, W.K.; Shim, J.-J. High-performance supercapacitors fabricated with activated carbon derived from lotus calyx biowaste. *Renew. Energy* **2022**, *189*, 587–600. [[CrossRef](#)]
95. Liang, T.; Hou, R.; Dou, Q.; Zhang, H.; Yan, X. The Applications of Water-in-Salt Electrolytes in Electrochemical Energy Storage Devices. *Adv. Funct. Mater.* **2021**, *31*, 2006749. [[CrossRef](#)]
96. Wang, Z.; Yun, S.; Wang, X.; Wang, C.; Si, Y.; Zhang, Y.; Xu, H. Aloe peel-derived honeycomb-like bio-based carbon with controllable morphology and its superior electrochemical properties for new energy devices. *Ceram. Int.* **2019**, *45*, 4208–4218. [[CrossRef](#)]
97. Surya, K.; Michael, M.S. Hierarchical porous activated carbon prepared from biowaste of lemon peel for electrochemical double layer capacitors. *Biomass Bioenergy* **2021**, *152*, 106175. [[CrossRef](#)]
98. Yao, S.; Zhang, Z.; Wang, Y.; Liu, Z.; Li, Z. Simple one-pot strategy for converting biowaste into valuable graphitized hierarchically porous biochar for high-efficiency capacitive storage. *J. Energy Storage* **2021**, *44*, 103259. [[CrossRef](#)]
99. Quan, H.; Tao, W.; Wang, Y.; Chen, D. Enhanced supercapacitor performance of *Camellia oleifera* shell derived hierarchical porous carbon by carbon quantum dots. *J. Energy Storage* **2022**, *55*, 105573. [[CrossRef](#)]
100. Vinayagam, M.; Suresh Babu, R.; Sivasamy, A.; Ferreira de Barros, A.L. Biomass-derived porous activated carbon from *Syzygium cumini* fruit shells and *Chrysopogon zizanioides* roots for high-energy density symmetric supercapacitors. *Biomass Bioenergy* **2020**, *143*, 105838. [[CrossRef](#)]
101. Sun, Y.; Xu, D.; Wang, S. Self-assembly of biomass derivatives into multiple heteroatom-doped 3D-interconnected porous carbon for advanced supercapacitors. *Carbon* **2022**, *199*, 258–267. [[CrossRef](#)]
102. Xu, X.; Sielicki, K.; Min, J.; Li, J.; Hao, C.; Wen, X.; Chen, X.; Mijowska, E. One-step converting biowaste wolfberry fruits into hierarchical porous carbon and its application for high-performance supercapacitors. *Renew. Energy* **2022**, *185*, 187–195. [[CrossRef](#)]
103. Cao, L.; Li, H.; Xu, Z.; Zhang, H.; Ding, L.; Wang, S.; Zhang, G.; Hou, H.; Xu, W.; Yang, F.; et al. Comparison of the heteroatoms-doped biomass-derived carbon prepared by one-step nitrogen-containing activator for high performance supercapacitor. *Diamond. Relat. Mater.* **2021**, *114*, 108316. [[CrossRef](#)]
104. Liu, Y.; Tan, H.; Tan, Z.; Cheng, X. Rice husk derived capacitive carbon prepared by one-step molten salt carbonization for supercapacitors. *J. Energy Storage* **2022**, *55*, 105437. [[CrossRef](#)]

105. Rani, M.U.; Nanaji, K.; Rao, T.N.; Deshpande, A.S. Corn husk derived activated carbon with enhanced electrochemical performance for high-voltage supercapacitors. *J. Power Source* **2020**, *471*, 228387. [CrossRef]
106. Elmouwahidi, A.; Bailón-García, E.; Pérez-Cadenas, A.F.; Maldonado-Hódar, F.J.; Carrasco-Marín, F. Activated carbons from KOH and H₃PO₄-activation of olive residues and its application as supercapacitor electrodes. *Electrochim. Acta* **2017**, *229*, 219–228. [CrossRef]
107. Coal—Statistical Review of World Energy 2021-BP. Available online: <https://www.bp.com/content/dam/bp/business-sites/en/global/corporate/pdfs/energy-economics/statistical-review/bp-stats-review-2021-full-report.pdf> (accessed on 11 July 2023).
108. Nalbandian, H.; House, P. *Non-Fuel Uses of Coal*; IEA Coal Research Center: London, UK, 2014.
109. Voncken, J. The Origin and Classification of Coal. In *Geology of Coal Deposits of South Limburg, The Netherlands*; Springer: Berlin/Heidelberg, Germany, 2020; pp. 25–40.
110. Zhao, X.-Y.; Huang, S.-S.; Cao, J.-P.; Xi, S.-C.; Wei, X.-Y.; Kamamoto, J.; Takarada, T. KOH activation of a HyperCoal to develop activated carbons for electric double-layer capacitors. *J. Anal. Appl. Pyrolysis* **2014**, *105*, 116–121. [CrossRef]
111. Shi, M.; Xin, Y.; Chen, X.; Zou, K.; Jing, W.; Sun, J.; Chen, Y.; Liu, Y. Coal-derived porous activated carbon with ultrahigh specific surface area and excellent electrochemical performance for supercapacitors. *J. Alloys Compd.* **2021**, *859*, 157856. [CrossRef]
112. Peng, Z.; Guo, Z.; Chu, W.; Wei, M. Facile synthesis of high-surface-area activated carbon from coal for supercapacitors and high CO₂ sorption. *RSC Adv.* **2016**, *6*, 42019–42028. [CrossRef]
113. Bora, M.; Tamuly, J.; Maria Benoy, S.; Hazarika, S.; Bhattacharjya, D.; Saikia, B.K. Highly scalable and environment-friendly conversion of low-grade coal to activated carbon for use as electrode material in symmetric supercapacitor. *Fuel* **2022**, *329*, 125385. [CrossRef]
114. Dong, D.; Zhang, Y.; Xiao, Y.; Wang, T.; Wang, J.; Romero, C.E.; Pan, W.-P. High performance aqueous supercapacitor based on nitrogen-doped coal-based activated carbon electrode materials. *J. Colloid Interface Sci.* **2020**, *580*, 77–87. [CrossRef]
115. Qin, B.; Wang, Q.; Zhang, X.; Xie, X.; Jin, L.E.; Cao, Q. One-pot synthesis of interconnected porous carbon derived from coal tar pitch and cellulose for high-performance supercapacitors. *Electrochim. Acta* **2018**, *283*, 655–663. [CrossRef]
116. Cheng, J.; Lu, Z.; Zhao, X.; Chen, X.; Liu, Y. Green needle coke-derived porous carbon for high-performance symmetric supercapacitor. *J. Power Source* **2021**, *494*, 229770. [CrossRef]
117. Liu, H.; Song, H.; Hou, W.; Chang, Y.; Zhang, Y.; Li, Y.; Zhao, Y.; Han, G. Coal tar pitch-based hierarchical porous carbons prepared in molten salt for supercapacitors. *Mater. Chem. Phys.* **2021**, *265*, 124491. [CrossRef]
118. Liu, Y.; Qu, X.; Huang, G.; Xing, B.; Fan, Y.; Zhang, C.; Cao, Y. Microporous carbon derived from anthracite as supercapacitor electrodes with commercial level mass loading. *J. Energy Storage* **2021**, *43*, 103200. [CrossRef]
119. Dong, D.; Zhang, Y.; Wang, T.; Wang, J.; Romero, C.E.; Pan, W.-p. Enhancing the pore wettability of coal-based porous carbon as electrode materials for high performance supercapacitors. *Mater. Chem. Phys.* **2020**, *252*, 123381. [CrossRef]
120. Yang, N.; Ji, L.; Fu, H.; Shen, Y.; Wang, M.; Liu, J.; Chang, L.; Lv, Y. Hierarchical porous carbon derived from coal-based carbon foam for high-performance supercapacitors. *Chin. Chem. Lett.* **2022**, *33*, 3961–3967. [CrossRef]
121. Mastragostino, M.; Arbizzani, C.; Paraventi, R.; Zanelli, A. Polymer selection and cell design for electric-vehicle supercapacitors. *J. Electrochem. Soc.* **2000**, *147*, 407. [CrossRef]
122. Wang, G.; Zhang, L.; Zhang, J. A review of electrode materials for electrochemical supercapacitors. *Chem. Soc. Rev.* **2012**, *41*, 797–828. [CrossRef] [PubMed]
123. González, A.; Goikolea, E.; Barrena, J.A.; Mysyk, R. Review on supercapacitors: Technologies and materials. *Renew. Sustain. Energy Rev.* **2016**, *58*, 1189–1206. [CrossRef]
124. Sajjad, M.; Khan, M.I.; Cheng, F.; Lu, W. A review on selection criteria of aqueous electrolytes performance evaluation for advanced asymmetric supercapacitors. *J. Energy Storage* **2021**, *40*, 102729. [CrossRef]
125. Huang, J.; Yuan, K.; Chen, Y. Wide Voltage Aqueous Asymmetric Supercapacitors: Advances, Strategies, and Challenges. *Adv. Funct. Mater.* **2021**, *32*, 2108107. [CrossRef]
126. Xu, C.; Yang, G.; Wu, D.; Yao, M.; Xing, C.; Zhang, J.; Zhang, H.; Li, F.; Feng, Y.; Qi, S. Roadmap on Ionic Liquid Electrolytes for Energy Storage Devices. *Chem. Asian J.* **2021**, *16*, 549–562. [CrossRef]
127. Bhat, T.; Patil, P.; Rakhi, R. Recent trends in electrolytes for supercapacitors. *J. Energy Storage* **2022**, *50*, 104222. [CrossRef]
128. Abdallah, T.; Lemordant, D.; Claude-Montigny, B. Are room temperature ionic liquids able to improve the safety of supercapacitors organic electrolytes without degrading the performances? *J. Power Source* **2012**, *201*, 353–359. [CrossRef]
129. Wasserscheid, P.; Keim, W. Ionic liquids—New “solutions” for transition metal catalysis. *Angew. Chem. Int. Ed.* **2000**, *39*, 3772–3789. [CrossRef]
130. Welton, T. Room-temperature ionic liquids. Solvents for synthesis and catalysis. *Chem. Rev.* **1999**, *99*, 2071–2084. [CrossRef]
131. Liu, H.; Yu, H. Ionic liquids for electrochemical energy storage devices applications. *J. Mater. Sci. Technol.* **2019**, *35*, 674–686. [CrossRef]
132. Stettner, T.; Balducci, A. Protic ionic liquids in energy storage devices: Past, present and future perspective. *Energy Storage Mater.* **2021**, *40*, 402–414. [CrossRef]
133. Galiński, M.; Lewandowski, A.; Stępnia, I. Ionic liquids as electrolytes. *Electrochim. Acta* **2006**, *51*, 5567–5580. [CrossRef]
134. Suo, L.; Borodin, O.; Gao, T.; Olguin, M.; Ho, J.; Fan, X.; Luo, C.; Wang, C.; Xu, K. “Water-in-salt” electrolyte enables high-voltage aqueous lithium-ion chemistries. *Science* **2015**, *350*, 938–943. [CrossRef]
135. Eftekhari, A. High-energy aqueous lithium batteries. *Adv. Energy Mater.* **2018**, *8*, 1801156. [CrossRef]

136. Bu, X.; Su, L.; Dou, Q.; Lei, S.; Yan, X. A low-cost “water-in-salt” electrolyte for a 2.3 V high-rate carbon-based supercapacitor. *J. Mater. Chem. A* **2019**, *7*, 7541–7547. [[CrossRef](#)]
137. Lannelongue, P.; Bouchal, R.; Mourad, E.; Bodin, C.; Olarte, M.; Le Vot, S.; Favier, F.; Fontaine, O. “Water-in-Salt” for supercapacitors: A compromise between voltage, power density, energy density and stability. *J. Electrochem. Soc.* **2018**, *165*, A657. [[CrossRef](#)]
138. Suo, L.; Han, F.; Fan, X.; Liu, H.; Xu, K.; Wang, C. “Water-in-Salt” electrolytes enable green and safe Li-ion batteries for large scale electric energy storage applications. *J. Mater. Chem. A* **2016**, *4*, 6639–6644. [[CrossRef](#)]
139. Sun, W.; Suo, L.; Wang, F.; Eidson, N.; Yang, C.; Han, F.; Ma, Z.; Gao, T.; Zhu, M.; Wang, C. “Water-in-Salt” electrolyte enabled LiMn₂O₄/TiS₂ Lithium-ion batteries. *Electrochem. Commun.* **2017**, *82*, 71–74. [[CrossRef](#)]
140. Dou, Q.; Lei, S.; Wang, D.-W.; Zhang, Q.; Xiao, D.; Guo, H.; Wang, A.; Yang, H.; Li, Y.; Shi, S. Safe and high-rate supercapacitors based on an “acetonitrile/water in salt” hybrid electrolyte. *Energy Environ. Sci.* **2018**, *11*, 3212–3219. [[CrossRef](#)]
141. Lukatskaya, M.R.; Feldblyum, J.I.; Mackanic, D.G.; Lissel, F.; Michels, D.L.; Cui, Y.; Bao, Z. Concentrated mixed cation acetate “water-in-salt” solutions as green and low-cost high voltage electrolytes for aqueous batteries. *Energy Environ. Sci.* **2018**, *11*, 2876–2883. [[CrossRef](#)]
142. Tian, Z.; Deng, W.; Wang, X.; Liu, C.; Li, C.; Chen, J.; Xue, M.; Li, R.; Pan, F. Superconcentrated aqueous electrolyte to enhance energy density for advanced supercapacitors. *Funct. Mater. Lett.* **2017**, *10*, 1750081. [[CrossRef](#)]
143. Maier, R.M.; Gentry, T.J. Microorganisms and organic pollutants. In *Environmental Microbiology*; Elsevier: Amsterdam, The Netherlands, 2015; pp. 377–413.
144. El Halimi, M.S.; Poli, F.; Mancuso, N.; Olivieri, A.; Mattioli, E.J.; Calvaresi, M.; Chafik, T.; Zanelli, A.; Soavi, F. Circumneutral concentrated ammonium acetate solution as water-in-salt electrolyte. *Electrochim. Acta* **2021**, *389*, 138653. [[CrossRef](#)]

Disclaimer/Publisher’s Note: The statements, opinions and data contained in all publications are solely those of the individual author(s) and contributor(s) and not of MDPI and/or the editor(s). MDPI and/or the editor(s) disclaim responsibility for any injury to people or property resulting from any ideas, methods, instructions or products referred to in the content.